

Slip flow of an optically thin radiating non-gray couple stress fluid past a stretching sheet

Sanatan Das*¹, Akram Ali¹ and Rabindra Nath Jana²

¹Department of Mathematics, University of Gour Banga, Malda 732 103, India

²Department of Applied Mathematics, Vidyasagar University, Midnapore 721 102, India

PAPER INFO

History:

Submitted 1 January 2016

Revised 3 April 2016

Accepted 22 May 2016

Keywords:

slip flow

couple stress fluid

stretching sheet thermal

radiation viscous

dissipation

ABSTRACT

This study addresses the combined effects of couple stresses, thermal radiation, viscous dissipation and slip condition on a free convective flow of a viscous incompressible couple stress fluid induced by a vertical stretching sheet. Cogley-Vincenti-Gilles equilibrium model is employed to include the effects of thermal radiation in the study. The governing boundary layer equations are transformed into a system of nonlinear differential equations, and solved numerically using the Runge-Kutta fourth-order method with shooting technique. Numerical results are obtained for the fluid velocity, temperature as well as the shear stress and rate of heat transfer. Then, the effects of the pertinent parameters on these quantities are examined. It is found that both the fluid velocity and temperature reduce in the presence of thermal radiation. Increasing the values of the couple stress parameter thickens the momentum boundary layer. The slip parameter greatly influences the fluid flow and shear stress on the surface of the stretching sheet.

© 2016 Published by Semnan University Press. All rights reserved.

Introduction

During recent years the study of convection heat and mass transfer in non-Newtonian fluids has received much attention and this is because the traditional Newtonian fluids can not precisely describe the characteristics of the real fluids. The couple-stress fluids introduced by Stokes [1-2] have distinct features, such as the presence of couple stresses, body couples and non-symmetric stress tensor. The couple-stress fluid theory presents models for the fluids whose microstructure is of mechanical significance. The effect of very small microstructure in a fluid can be felt if the characteristic geometric dimension of the problem considered is of the same order of magnitude as the size of the microstructure. The main feature of the couple stresses is that they introduce a size-dependent effect. Classical continuum mechanics neglects the size effect of material particles within the continua. This is consistent with ignoring the rotational interaction among particles, which results

in symmetry of the force-stress tensor. However, in some important cases such as fluid flow with suspended particles, it can not be true and a size-dependent couple-stress theory is needed. The spin field, due to microrotation of freely suspended particles, set up an antisymmetric stress, known as couple-stress, leading to a couple-stress fluid. These fluids are capable of describing various types of lubricants, blood, suspension fluids, etc. The study of couple-stress fluids has a wide range of applications in various industries such as the extrusion of polymer fluids, solidification of liquid crystals, cooling of metallic plate in a bath and colloidal solutions, etc. Convective flows with radiation are also applied in many industrial processes such as heating and cooling of chambers, energy processes, evaporation from large reservoirs, solar power technology and space vehicle re-entry.

The boundary layer flow over a stretching sheet in a uniform stream of fluid has been studied

extensively in fluid mechanics. A large number of studies has been done in the area of boundary layer flow over a continuous stretching surface with regard to its numerous industrial and engineering applications. It occurs frequently in manufacturing involving hot metal rolling, wire drawing, producing glass-fiber, producing paper, drawing of plastic films, manufacturing foods, crystal growing, liquid films in condensation process and metal spinning, as well as metal and polymer extrusion processes (Fisher [3]). The flow and heat transfer over a stretching sheet have tremendous industrial applications, for instance, in the extrusion of a polymer sheet from a die. In the process of manufacturing such sheets, the melt issues from a slit are subsequently stretched. The rates of stretching and cooling have a significant influence on the quality of the final product with desired characteristics. The aforementioned processes involve cooling of a molten liquid by drawing it into a cooling system. The desired properties for the product of such process mainly depend on two characteristics: the first is the cooling liquid used and the other is the rate of stretching. The liquids of non-Newtonian characteristics can be chosen for as a cooling liquid as their flow and hence the heat transfer rate can be regulated through some external means. The optimal rate of stretching is important, as rapid stretching results in sudden solidification, thereby destroying the properties expected from the product.

After the pioneering study of Sakiadis [4] and Crane [5], a large number of studies on a stretching sheet have been published by considering various governing parameters such as suction/injection, porosity, magnetic field parameter, and radiation with different types of fluids such as Newtonian, non-Newtonian, polar, and couple stress fluids. However, the abundant literature on the boundary layer flow over a stretching sheet is limited to Newtonian and some non-Newtonian fluids flow with traditional no-slip flow boundary condition over various stretching geometries such as linear and non-linear stretching sheet and a little attention is given to stretching sheet with slip boundary condition. However, the fluids with micro-scale or nano-scale dimensions have flow behavior that greatly differs from the traditional fluid flow characteristics and belongs to the slip flow regime. For the flow in the slip regime, the fluid motion still obeys the Navier-Stoke's equations, but with slip velocity, temperature and concentration boundary conditions. For instance, the flow in many applications of micro/nano systems such as hard disk drive, micro-pump, micro-valve and micro-nozzles is in slip transition regime, which is characterized by slip boundary at the wall.

Several researchers have considered various aspects of momentum and heat transfer characteristics in boundary layer flow over a stretching boundary (Gupta and Gupta [6], Rajagopal

et al. [7], Siddappa and Abel [8], Andersson [9], Kumaran and Ramanaiah [10], Wang [11] and Cortell [12]). Flow of elastico-viscous fluid induced by a stretching sheet with slip has been presented by Ariel et al. [13]. Akyildiz et al. [14] have discussed the diffusion of chemically reactive species in a porous medium over a stretching sheet. Wang [15] have made an analysis of viscous flow due to a stretching sheet with surface slip and suction. Fang et al. [16-17] have obtained the exact solution of an MHD slip flow over a stretching sheet. The thermal boundary layers over a shrinking sheet have been analytically studied by Fang and Zhang [18]. The heat transfer characteristics in a visco-elastic boundary layer flow over a stretching sheet have been analyzed by Arnold et al. [19]. Shantha et al. [20] have presented the free convection flow of a conducting couple stress fluid in a porous medium. Srinivasacharya and Kaladhar [21] have conducted a study of a mixed convection flow of couple stress fluid in a non-darcy porous medium with Soret and Dufour effects. The second-order slip flow and heat transfer over a stretching sheet with non-linear Navier boundary condition have been numerically investigated by Nandeppanavar et al. [22]. Singh and Makinde [23] have studied an MHD slip flow of viscous fluid over an isothermal reactive stretching sheet. Hayat et al. [24] have presented the stagnation-point flow of couple stress fluid with melting heat transfer. Turkyilmazoglu [25] has obtained an exact solution for two-dimensional laminar flow over a continuously stretching or shrinking sheet in an electrically conducting quiescent couple stress fluid. The MHD flow and heat transfer of an exponential stretching sheet in a Boussinesq-Stokes suspension have been examined by Siddheshwar et al. [26]. Salema et al. [27] have studied the hydromagnetic flow of Cu-water nanofluid past a moving wedge with viscous dissipation. Zhu et al. [28] have presented the second-order slip MHD flow and heat transfer of nanofluids with thermal radiation and chemical reaction. Sheikholeslami et al. [29] have investigated the magnetic nanofluid forced convective heat transfer with variable magnetic field using two-phase model. The effect of non-uniform magnetic field on forced convection heat transfer of Fe_3O_4 -water nanofluid has been examined by Sheikholeslami et al. [30]. Kandelousi [31] has studied the effect of spatially variable magnetic field on ferrofluid flow and heat transfer considering constant heat flux boundary condition. Sheikholeslami and Ganji [32] have presented the nanofluid flow and heat transfer between parallel plates considering Brownian motion using DTM. The effect of thermal radiation on a magnetohydrodynamic nanofluid flow and heat transfer has been examined by Sheikholeslami et al. [33]. Sheikholeslami [34] has presented the forced convective heat transfer in a semi-annulus under the influence of a variable magnetic field.

In the present study, the free convective slip flow induced by a vertical linearly stretching sheet in couple stress fluid is presented in the presence of thermal radiation by adopting the Cogley- Vincenti-Gilles equilibrium model introduced by Cogley et al. [35]. The sheet surface is isothermal. The partial differential equations governing the flow are transformed into ordinary differential equations using the similarity transformation and are numerically solved. The interplay between pertinent parameters is explained using graphs.

1. Mathematical Formulation

A steady slip flow of a viscous incompressible couple stress fluid over an isothermal vertical linearly stretching sheet is considered. A Cartesian co-ordinate system with x-axis along the sheet is chosen and the y-axis is normal to it (see Fig.1). The sheet stretches in its own plane with the velocity $U_w = ax$, $a(>0)$ being a constant known as stretching rate. The sheet surface is heated by the temperature T_w while the temperature of the ambient cold fluid is T_∞ . All the fluid properties are assumed to be constant except the density in the buoyancy term of the momentum equation.

The Stokes constitutive model for the couple stresses is used. Under the usual Boussinesq's approximation, the free convection flow of a radiating couple stress fluid is governed by the following system of equations:

$$\frac{\partial u}{\partial x} + \frac{\partial v}{\partial y} = 0, \tag{1}$$

$$u \frac{\partial u}{\partial x} + v \frac{\partial u}{\partial y} = \nu \frac{\partial^2 u}{\partial y^2} - \nu^* \frac{\partial^4 u}{\partial y^4} + g\beta(T - T_\infty), \tag{2}$$

$$\rho c_p \left(u \frac{\partial T}{\partial x} + v \frac{\partial T}{\partial y} \right) = k \frac{\partial^2 T}{\partial y^2} - \frac{\partial q_r}{\partial y} + \mu \left(\frac{\partial u}{\partial y} \right)^2 \tag{3}$$

Where u and v are the velocity components along the x and y-directions, respectively, T is the temperature of the fluid, g is the acceleration due to gravity, μ : the dynamic viscosity of the fluid, ν : the kinematic viscosity, ν^* : the couple stress viscosity, ρ : the fluid density, k : the thermal conductivity, β : the thermal expansion coefficient, c_p : the specific heat at constant pressure and q_r : the radiative heat flux. The asymptotical case as $\nu^* \rightarrow 0$ which corresponds to the purely Newtonian case. The boundary conditions are the following:

Where L denotes the slip coefficient and T_w is the temperature of the sheet. When $L = 0$, the no-slip condition is recovered.

It has been shown by Cogley et al. that in the optically thin limit for a non-gray gas near equilibrium, the following relation holds:

$$u = U_w(x) = ax + L \left(\frac{\partial u}{\partial y} \right), \quad v = 0, \quad \frac{\partial^2 u}{\partial y^2} = 0, \tag{4}$$

$$T = T_w \text{ at } y = 0, u \rightarrow 0,$$

$$\frac{\partial^2 u}{\partial y^2} \rightarrow 0, \quad T \rightarrow T_\infty \text{ as } y \rightarrow \infty,$$

$$\frac{\partial q_r}{\partial y} = 4(T - T_\infty) \int_0^\infty K_{\lambda^*} \left(\frac{\partial e_{\lambda^*} p}{\partial T} \right) d\lambda^*, \tag{5}$$

Where K_{λ^*} is the absorption coefficient, λ^* is the wave length, $e_{\lambda^*} p$ is the Planck's function and the subscript 'w' indicates that all quantities have been evaluated at the temperature T_w which is the temperature of the stretching sheet. Thus, our study is limited to small difference of surface temperature to the fluid temperature. Greif et al. [36] show that for an optically thin limit, the fluid does not absorb its own emitted radiation, it means that there is no self-absorption, but the fluid does absorb radiation emitted by the boundaries. The treatments to the radiative heating are either in the limit where photon mean free paths are very small, called optically thick or very long, called optically thin. At high temperature the presence of thermal radiation alters the distribution of temperature in the boundary layer, which in turn affects the heat transfer at the channel walls.

On the use of equation (5), the equation (3) becomes

$$\rho c_p \left(u \frac{\partial T}{\partial x} + v \frac{\partial T}{\partial y} \right) = k \frac{\partial^2 T}{\partial y^2} -$$

$$4(T - T_\infty) I + \mu \left(\frac{\partial u}{\partial y} \right)^2,$$

Where

$$I = \int_0^\infty K_{\lambda^*} \left(\frac{\partial e_{\lambda^*} p}{\partial T} \right) d\lambda^*. \tag{7}$$

The continuity equation (1) is satisfied by introducing a stream function $\psi(x, y)$ such as

$$u = \frac{\partial \psi}{\partial y}, \quad v = -\frac{\partial \psi}{\partial x}. \tag{8}$$

The following similarity variables are also introduced

$$\eta = y \sqrt{\frac{a}{\nu}}, \psi = \sqrt{av} x f(\eta), \theta = \frac{T - T_\infty}{T_w - T_\infty}, \tag{9}$$

Where η is the independent similarity variable, $f(\eta)$ is the non-dimensional stream function and $\theta(\eta)$ is the non-dimensional fluid temperature. Substituting the equation (9) into equations (2) and (6), we obtain the following ordinary differential equations:

$$C^2 f^{(V)} - f''' - f f'' + f'^2 - Gr\theta = 0, \tag{10}$$

$$\theta' + Pr f \theta' + Pr Ec f'^2 - R\theta = 0, \tag{11}$$

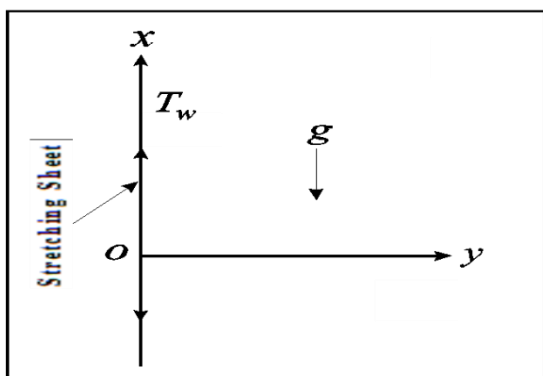


Fig. 1 The geometry of the problem

Where $R = \frac{4I\nu}{ka}$ is the radiation parameter,

$C^2 = \frac{\nu^*}{\nu a^2}$ is the couple stress parameter,

$Ec = \frac{U_w^2}{c_p(T_w - T_\infty)}$ is the Eckert number,

$Gr = \frac{g\beta(T_w - T_\infty)}{aU_w(x)}$ is the Grashof number that

approximates the ratio of the buoyancy force to the viscous force acting on a fluid and $Pr = \frac{\rho\nu c_p}{k}$ is

the Prandtl number which measures the ratio of momentum diffusivity to the thermal diffusivity. The corresponding boundary conditions are

$$\begin{aligned} f(0) &= 0, f'(0) = 1 + \gamma f''(0), \\ f''(0) &= 0, \theta(0) = 1, \\ f'(\infty) &\rightarrow 0, f''(\infty) \rightarrow 0, \theta(\infty) \rightarrow 0, \end{aligned} \tag{12}$$

Where $\gamma = L\sqrt{\frac{a}{\nu}}$ is the velocity slip parameter. The no-slip case is recovered for $\lambda = 0$. In the absence of thermal radiation ($R = 0$) and neglecting viscous dissipation ($Ec = 0$) and slip condition ($\lambda = 0$), the

present problem reduces to the problem considered by Siddheshwar et al. [26]. It is observed that the trends of the velocity profiles are similar in the absence of Chandrasekhar's number ($Q = 0$) as well as heat source/sink ($\lambda = 0$) in the case of the prescribed surface temperature.

2. Numerical Solution

It is well-known that most boundary layer transmission problems are described by a set of nonlinear partial differential equations. However, due to the strongly nonlinear and unconventional nature of these problems, the solving processes are extraordinarily complex, and the effective solutions are hardly obtained. Recently, various methods have been tried to solve these problems. The non-dimensional ordinary differential equations (10) and (11) with boundary conditions (12) are solved numerically. The highly nonlinear momentum boundary layer equation and the thermal boundary layer equation are converted into similarity equations and then solved numerically using the modified fourth-order Rung-Kutta method with shooting technique [37]. Rung-Kutta method is the fourth-order method meaning that the local truncation error is of order $o(\Delta\eta)^5$ whereas the total accumulated error is of order $o(\Delta\eta)^4$. This is a usual case that, the truncation error also includes discretization error, which is the error that arises from taking the finite number of steps in the computation to approximate an infinite process. The resulting higher order ordinary differential equations are reduced to first-order differential equations by letting

$$\begin{aligned} x_1 &= f, x_2 = f', x_3 = f'', \\ x_4 &= f''', x_5 = f^{(IV)}, x_6 = \theta, x_7 = \theta'. \end{aligned} \tag{13}$$

Thus, the corresponding coupled higher order non-linear differential equations become:

$$\begin{aligned} x_1' &= x_2, \\ x_2' &= x_3, \\ x_3' &= x_4, \\ x_4' &= x_5, \\ x_5' &= \frac{1}{C^2}[x_4 + x_1 x_3 - x_2^2 + Gr x_6], \\ x_6' &= x_7, \\ x_7' &= R x_6 - Pr x_1 x_7 - Pr Ec x_3^2 \end{aligned} \tag{14}$$

With the boundary conditions:

$$\begin{aligned}
 x_1(0) &= 0, x_2(0) = 1 + \gamma x_3(0), \\
 x_3(0) &= b, x_4(0) = 0, \\
 x_5(0) &= c, x_6(0) = 1, x_7(0) = d,
 \end{aligned}
 \tag{15}$$

Where b , c and d are unknown which are to be determined as a part of the numerical solution. In the shooting method, the unspecified initial conditions b , c and d are assumed and equation (14) is integrated numerically as an initially valued problem to a given terminal point. The accuracy of the assumed missing initial condition is checked by comparing the calculated value of the dependent variable at the terminal point with its given value there. If a difference exists, the improved values of the missing initial conditions must be obtained and the process is repeated. The numerical computations are done by MATLAB bvp4c routine. The step-size is taken as $\eta = 0.01$. The process is repeated until we get the results correct up to the desired accuracy of 10^{-6} level.

3. Results and Discussion

In order to get a physical insight of the problem, we illustrate the effects of the pertinent parameters, namely couple stress parameter C^2 , Grashof number Gr , radiation parameter R , Prandtl number Pr , Eckert number Ec and slip parameter γ on the fluid velocity, temperature, shear stress and rate of heat transfer. Prandtl number (Pr) is chosen as the values ranging from $0.72 \leq Pr \leq 7.1$ which are the most encountered fluids used in industries. $Ec = 0$ presents no Joule and viscous heating. For a large value of slip parameter γ which corresponds to a very small x at the leading edge, the boundary layer assumption is not appropriate, i.e. the boundary layer equations become inaccurate. Also, the Knudsen number is greater than 0.1 for a large γ and hence the Navier-Stokes equation fails to model the flow regime. We therefore limit the discussion in this study to a relatively small range of γ from 0 to 2.5 as this range exhibits the slip flow region. The default values of the other parameters are mentioned in the description of the respective figures.

4.1. Effects of parameters on stream function

Figs.2-3 present the stream function for several values of Grashof number Gr and Eckert number Ec . It is seen from these figures that the stream function increases with an increase in either Gr or Ec . Figs.4-6 reveals that the stream function decreases with an increase in either couple stress

parameter C or radiation parameter R or Prandtl number Pr .

4.2. Effects of parameters on velocity profiles

Figs.7-8 show that the fluid velocity increases with an increase in either Grashof number Gr or Eckert number Ec . Physically speaking, the Grashof number signifies the relative importance of buoyancy force to the viscous hydrodynamic force.

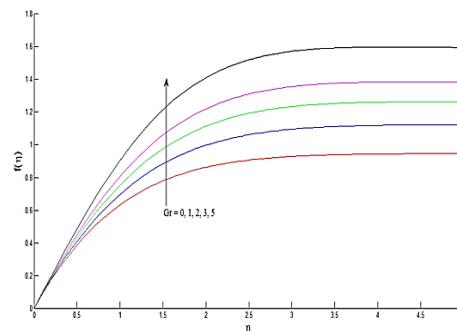


Fig. 2 The non-dimensional stream function for different Gr when $C = 0.5$, $R = 2$, $Gr = 5$, $Pr = 0.72$, $Ec = 0.5$ and $\gamma = 0.1$

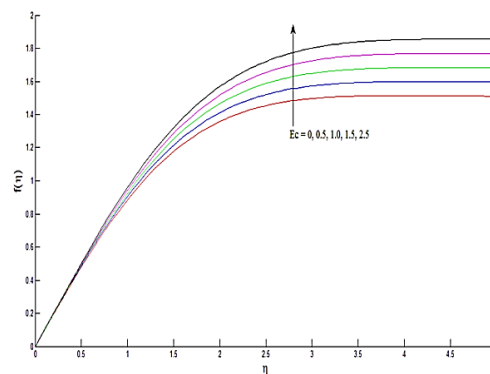


Fig. 3 The non-dimensional stream function for different Ec when $R = 2$, $Gr = 5$, $Pr = 0.72$, $C = 0.5$ and $\gamma = 0.1$

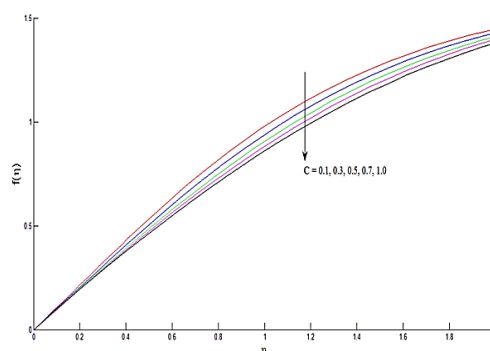


Fig. 4 The non-dimensional stream function for different C when $C = 0.5$, $R = 2$, $Gr = 5$, $Pr = 0.72$, $Ec = 0.5$ and $\gamma = 0.1$

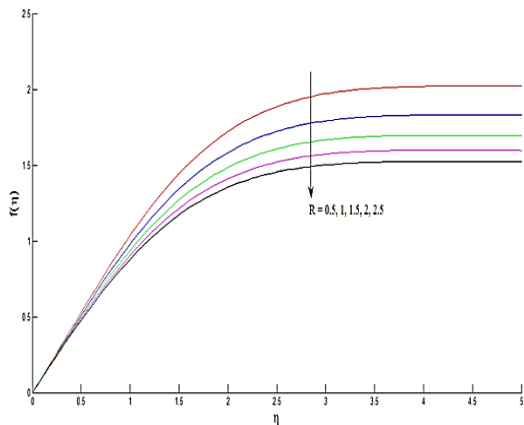


Fig.5 The non-dimensional stream function for different R when $C = 0.5$, $Gr = 5$, $Pr = 0.72$, $Ec = 0.5$ and $\gamma = 0.1$

Larger Grashof number indicates lower viscous effects in momentum equation. For higher values of Gr , the fluid velocity overshoots the sheet velocity in the regions close to the surface of the sheet. Physically, $Gr > 0$ means heating of the fluid by cooling the boundary surface. It is also revealed that the momentum boundary layer thickness reduces as the Grashof number Gr increases and it increases as the Eckert number Ec increases. The Eckert number Ec expresses the relationship between the kinetic energy in the flow and the enthalpy. It embodies the conversion of kinetic energy into internal energy by work done against the viscous fluid stresses. Greater viscous dissipative heat causes a rise in the fluid temperature and hence the fluid velocity enhances. Fig.9 reveals that the fluid velocity decreases near the sheet surface and increases away from the surface of the sheet with an increase in the couple stress parameter C . This means that the increasing values of C result in thickening of the momentum boundary layer. Expectedly, the couple stresses enhance the fluid's intermolecular cohesion. This increases the fluid's resistance to shear stress, resulting in a decrease in velocity. Fig.10 depicts the effects of the radiation parameter R on the velocity profile. The fluid velocity decreases for increasing the values of R . The thermal radiation has increased the momentum boundary layer thickness. Fig.11 presents the fluid velocity profiles for several values of Prandtl number Pr . The thickness of the momentum boundary layer is also greater. The reason for such a behavior is that an increase in the Prandtl number is due to an increase in the fluid viscosity, which makes the fluid thick, thus decreasing its velocity. It is seen from Fig.12 that the fluid velocity decreases with an increase in the slip parameter γ . Physically, when

slip occurs, the slipping fluid shows a decrease in the surface skin-friction between the fluid and the stretching sheet because not all the pulling force of the stretching sheet can be transmitted to the fluid. So, increasing the value of γ decreases the fluid velocity in the region of the boundary layer.

4.3. Effects of parameters on temperature profiles

Figs. 13-15 illustrate the temperature field against the coordinate η . The fluid temperature is the highest at the sheet and decreases asymptotically to zero far away from the sheet satisfying the boundary conditions. Figs. 13 and 14 present the profiles of the fluid temperature for several values of radiation parameter R and Prandtl number Pr .

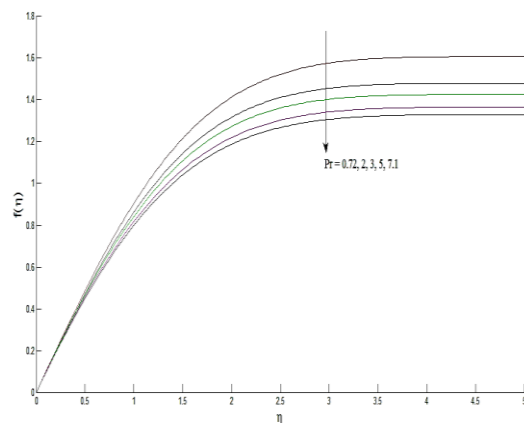


Fig.6 The non-dimensional stream function for different R when $C = 0.5$, $Gr = 5$, $Pr = 0.72$, $Ec = 0.5$ and $\gamma = 0.1$

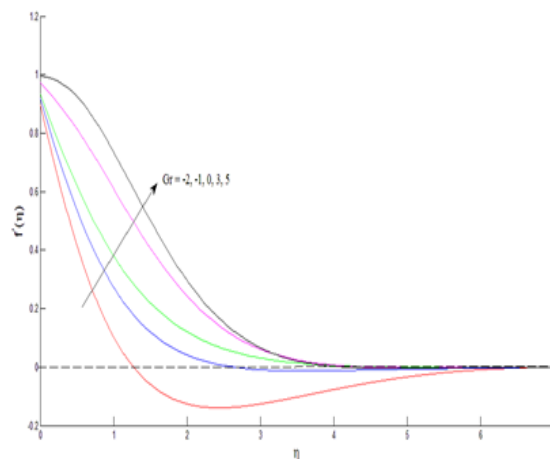


Fig.7 The velocity profile for different Gr when $C = 0.5$, $R = 2$, $Pr = 0.72$, $Ec = 0.5$ and $\gamma = 0.1$

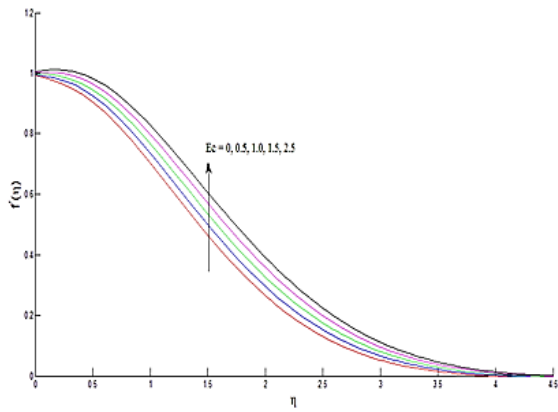


Fig.8 The velocity profile for different Ec when $R = 2$, $Gr = 5$, $Pr = 0.72$, $C = 0.5$ and $\gamma = 0.1$

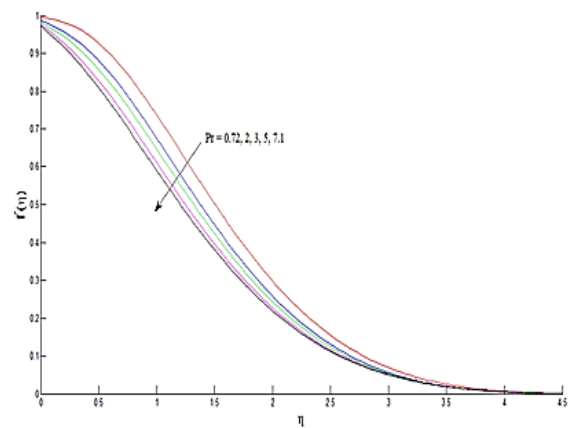


Fig.11 The velocity profile for different Pr when $C = 0.5$, $Gr = 5$, $R = 2$, $Ec = 0.5$ and $\gamma = 0.1$

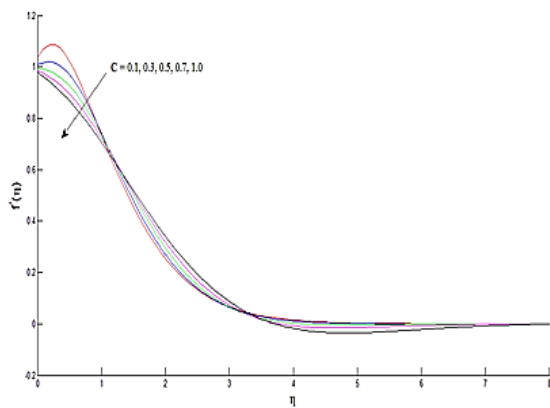


Fig. 9 The velocity profile for different C when $R = 2$, $Gr = 5$, $Pr = 0.71$, $Ec = 0.5$ and $\gamma = 0.1$

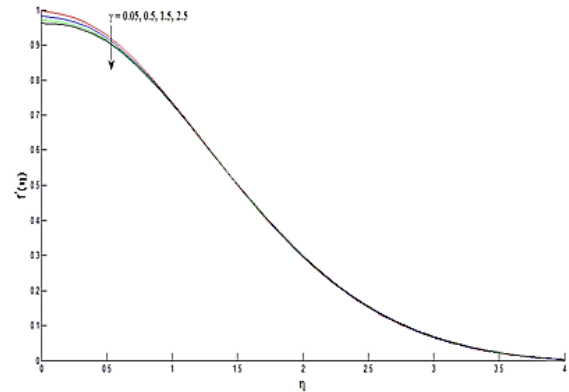


Fig.12 The velocity profile for different γ when $Gr = 5$, $Pr = 0.72$, $C = 0.5$, $R = 2$ and $Ec = 0.5$

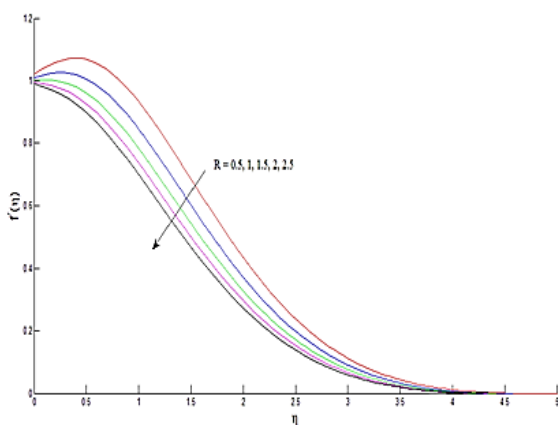


Fig.10: The velocity profile for different Pr when $Gr = 5$, $Pr = 0.72$, $C = 0.5$, $Ec = 0.5$ and $\gamma = 0.1$

An increase in the thermal radiation R causes a decrease in the fluid temperature within the boundary layer and consequently the thermal boundary layer thickness decreases as shown in Fig. 13. The temperature decreases with an increase in the radiation parameter as the release of heat energy from the flow region is also increased, resulting in a decrease in the fluid temperature. It is seen from Fig.14 that the fluid temperature decreases with an increase in the Prandtl number Pr . From this figure it is noticed that an increase in the Prandtl number results in a decrease in temperature. The reason is that the smaller values of the Prandtl number are equivalent to increasing thermal conductivity and therefore heat is capable of diffusing away from the heated surface more rapidly than at the higher values of Pr . Thus, the temperature falls more rapidly for water than for air and electrolyte solution. An increase in the Pr causes a decrease in the thermal boundary layer thickness. Fig. 15 illustrates the influence of Eckert number Ec on temperature in the boundary layer. The fluid temperature increases with an increase in the Eckert number Ec . The Eckert number is the ratio of the kinetic energy

of the flow to the boundary layer enthalpy differences. It represents the conversion of the kinetic energy into the internal energy by work done against the viscous fluid stresses. The positive Eckert number means cooling of the surface of the stretching sheet, i.e loss of heat from the surface of the stretching sheet to the fluid. Hence, greater viscous dissipative heat causes a rise in the fluid temperature. Furthermore, it can be observed that the thermal boundary layer thickness becomes thicker for the increased Eckert number. The maximum temperature occurs in the vicinity of the surface of the stretching sheet and then the temperature asymptotically approaches to zero in the free-stream region.

4.4. Effects of parameters on shear stress and rate of heat transfer

For engineering purposes, one is usually interested in the values of the shear stress (or skin friction) and the heat transfer rate. The shear stress is an important parameter in the heat transfer studies, since it is directly related to the heat transfer coefficient. The increased shear stress is generally viewed as a disadvantage in the technical applications, while the increased heat transfer can be exploited in some applications. Numerical values of the rate of heat transfer $-\theta'(0)$ and the shear stress $-f''(0)$ at the surface of the sheet $\eta = 0$ are entered in the Table 1 for several values of C , R , Gr , Pr , Ec and γ . The shear stress $-f''(0)$ reduces with an increase in C , Pr and Ec while it enhances with an increase in either R or Gr or γ .

This may be attributed to a rise in the velocity gradient at the surface of the sheet due to the buoyancy force. An increase in the shear stress is observed with an increase in the thermal radiation. As expected, a fall in the fluid temperature due to a rise in the thermal radiation enhances the fluid viscosity, leading to an increase in the shear stress. A decrease in shear stress is noticed as Eckert number Ec increases. This may be explained by stating that, an increase in the fluid temperature due to the viscous heating may decrease the fluid viscosity, since viscosity is temperature dependent. It is also concluded from Table 1 that both friction factor and surface heat flux reduce with an increase in the value of Pr . This is expected, since an increase in the value of Pr decreases the thermal diffusivity of the fluid and it also reduces the magnitude of the frictional force between the viscous layers. Consequently, the shear stress reduces. Physically, the negative value of $f''(0)$ means the stretching sheet exerts a drag force on the fluid and the positive value means the opposite.

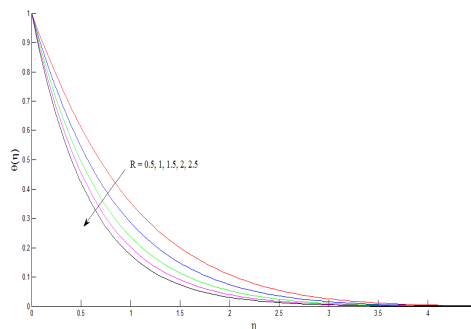


Fig.13 The temperature profile for different R when $Pr = 0.71$ and $Ec = 0.5$

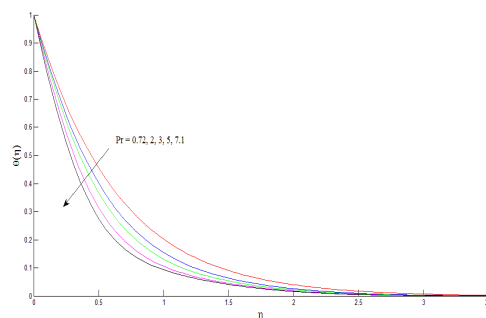


Fig.14 The temperature profile for different Pr when $R = 2$ and $Ec = 0.5$

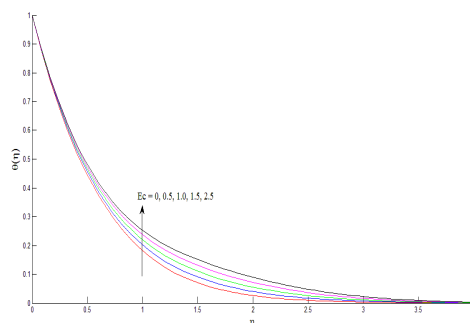


Fig.15 The temperature profile for different Ec when $R = 2$ and $Pr = 0.72$

It is seen from the Table 1 that the rate of heat transfer $-\theta'(0)$ increases for increasing values of C or R or Gr while it decreases for increasing values of Pr or Ec or γ . Due to the influence of thermal radiation, the temperature gradient increases which ultimately enhances the rate of heat transfer. Therefore, thermal radiation plays an important role in augmenting heat transfer rate or in other words it acts as a heat source. Thus, increasing the couple stresses and buoyancy force implies more intermolecular cohesion which generates more heat leading to an increase in the temperature which in turn causes an increase in the rate of heat transfer. On the other hand, $\theta'(0) < 0$ means the heat transfer takes place from the surface of the sheet to fluid.

Table 1. The rate of heat transfer $-\theta'(0)$ and shear stress $-f''(0)$ at the sheet $\eta = 0$.

C	R	Gr	Pr	Ec	γ	$-\theta'(0)$	$-f''(0)$
0.5	2	5	0.72	0.5	0.1	0.72691	1.55029
1.0	2	5	0.72	0.5	0.1	0.85015	1.53812
1.5	2	5	0.72	0.5	0.1	0.88136	1.53456
0.5	1					0.70732	1.27084
0.5	1.5					0.71752	1.41428
0.5	2					0.72691	1.55029
		3				0.82251	1.54067
		4				0.77469	1.54565
		5				0.72691	1.55029
			0.72			0.72691	1.55029
			2			0.72016	1.47688
			3			0.71505	1.42013
				0.0		0.74004	1.66408
				0.5		0.72691	1.55029
				1.0		0.71367	1.43867
					0.05	0.76583	1.54306
					0.5	0.51824	1.58209
					1.5	0.30328	1.60229

4. Conclusion

The boundary layer slip flow of couple- stress fluid past a vertical stretching sheet in the presence of thermal radiation has been numerically investigated. Using similarity transformations the governing equations of the problems are transformed into non-linear ordinary differential equations and solved for local similar solutions using shooting iteration technique together with fourth-order Runge-Kutta integration. The main results of the present study are summarized as follows:

- Fluid velocity enhances due to the buoyancy force and the momentum boundary layer thickness reduces due to an increase in the values of Grashof number .
- Fluid velocity is retarded due to the slip parameter.
- Fluid velocity reduces in the presence of thermal radiation.
- Effects of the thermal radiation and the Prandtl number are to decrease the thermal boundary layer thickness.
- The combination of the couple stress parameter, the slip parameter and the Eckert number greatly

affects the fluid flow and shear stress on the surface of the stretching sheet.

Acknowledgments

We thank the respected anonymous reviewer/s who contributed towards improvement of this paper.

References

- [1]. Stokes, V. K. (1966). Couple stresses in fluid. The Physics of Fluids 9(9), 1709-1715 .
- [2]. Stokes, V. K. (1984). Theories of Fluids with Microstructure: An Introduction, Springer Verlag, New York.
- [3]. Fischer, E.G. (1976). Extrusion of plastics. Wiley, New York, 1976.
- [4]. Sakiadis, B.C.(1961). Boundary layer behaviour on continuous solid surfaces: I boundary layer on a continuous flat surface. AICHE J. 7, 221-5.
- [5]. Crane, L.(1970). Flow past a stretching plate. Z. Angew. Math. Phys. 21, 645-7.
- [6]. Gupta, P.S., Gupta, A.S. (1977). Heat and mass transfer on a stretching sheet with suction or blowing. Canad. J. Chem. Engg. 55, 744-746.

- [7]. Rajagopal, K.R., Na, T.Y., Gupta, A.S.(1984). Flow of viscoelastic fluid due to a stretching sheet. *Rheol. Acta.* 23, 213-215.
- [8]. Siddappa, B., Abel, M. S.(1985). Non- Newtonian flow past a stretching surface, *Z. Angew. Math. Phys.* 36, 890-892.
- [9]. Andersson, H.I.(1992). MHD flow of a viscoelastic fluid past a stretching surface. *Acta Mech.* 95, 227-230.
- [10]. Kumaran, V., Ramanaiyah, G.(1996) A note on the flow over a stretching sheet. *Acta Mech.* 116, 229- 233.
- [11]. Wang, C.Y. (2002). Flow due to a stretching boundary with partial slip. An exact solution of the Navier–Stokes equations. *Chem. Eng. Sci.* 57, 3745–7.
- [12]. Cortell, R. (2007). Viscous flow and heat transfer over a nonlinearly stretching sheet. *Appl. Math. Comput.* 184 (2), 864-873.
- [13]. Ariel, P.D., Hayat, T., Asghar, S. (2006). The flow of an elastico-viscous fluid past a stretching sheet with slip. *Acta Mech.* 187, 29–36.
- [14]. Akyildiz, F.T., Bellout, H., Vajravelu, K.(2006). Diffusion of chemically reactive species in a porous medium over a stretching sheet. *J. Math. Anal, Appl.* 320, 322–39.
- [15]. Wang, C.Y.(2009). Analysis of viscous flow due to a stretching sheet with surface slip and suction. *Nonlinear Anal Real World Appl.* 10, 375–80.
- [16]. Fang, T., Zhang, J., Yao, S. (2009). Slip MHD viscous flow over a stretching sheet- An exact solution. *Comm. Nonlinear Num. Simu.* 14, 3731-3737.
- [17]. Fang, T., Zhang, J., Yao, S. (2010). Slip MHD viscous flow over a permeable shrinking sheet. *Chinese Phys. Lett.* 27, 124702.
- [18]. Fang, T.G., Zhang, J.(2010). Thermal boundary layers over a shrinking sheet: an analytical solution. *Acta Mech.* 209, 325–43.
- [19]. Arnold, J.C., Asir, A.A.,Somasundaram, S., Christopher, T. (2010). Heat transfer in a visco-elastic boundary layer flow over a stretching sheet. *Int. J. Heat Mass Transfer* 53, 1112–8.
- [20]. Shantha, G., Shanker, B. (2010). Free convection flow of a conducting couple stress fluid in a porous medium. *Int. J. Numer. Methods Heat Fluid Flow* 20, 250-264.
- [21]. Srinivasacharya, D., Kaladhar, K. (2012). Mixed convection flow of couple stress fluid in a non-darcy porous medium with Soret and Dufour effects. *J. Appl. Sci. Eng* 15, 415 -422.
- [22]. Nandeppanavar, M.M., Vajravelu, K., Abel, M.S., Siddalingappa, M. N.(2012). Second order slip flow and heat transfer over a stretching sheet with non-linear Navier boundary condition. *Int. J. Therm. Sci.* 58, 143–50.
- [23]. Singh, G., Makinde, O.D. (2013). MHD slip flow of viscous fluid over an isothermal reactive stretching sheet. *ANNALS of Faculty Engineering Hunedoara – Int. J. Engn.* Tome XI, 41-46.
- [24]. Hayat, T., Mustafa, M., Iqbal, Z., Alsaedi, A. (2013). Stagnation-point flow of couple stress fluid with melting heat transfer. *Appl. Math. Mech.-Eng.* Ed 34, 167-176.
- [25]. Turkyilmazoglu, M. (2014). Exact solutions for two-dimensional laminar flow over a continuously stretching or shrinking sheet in an electrically conducting quiescent couple stress fluid. *Int.J. Heat Mass Transfer* 72, 1-8.
- [26]. Siddheshwar, P.G., Sekhar, G.N., A. S. Chethan, A.S. (2014). MHD Flow and heat transfer of an exponential stretching sheet in a Boussinesq-Stokes suspension. *J. Appl. Fluid Mech.* 7(1), 169-176.
- [27]. Salem, A. M., Ismail, G. Fathy, R. (2014). Hydromagnetic flow of Cu- water nanofluid past a moving wedge with viscous dissipation. *Chin. Phys. B* 23(4), 044402.
- [28]. Zhu, J., Zheng, L., Zheng, L., Zhang, X. (2015). Second-order slip MHD flow and heat transfer of nanofluids with thermal radiation and chemical reaction. *Appl. Math. Mech. - Engl. Ed.*, 36(9), 1131-1146.
- [29]. Sheikholeslami, M., Rashidi, M.M. , Ganji, D.D. (2015). Numerical investigation of magnetic nanofluid forced convective heat transfer in existence of variable magnetic field using two phase model. *J. Molecular Liquids* 212, 117-126.
- [30]. Sheikholeslami, M., Rashidi, M.M., Ganji, D.D. (2015). Effect of non-uniform magnetic field on forced convection heat transfer of Fe₃O₄- water nanofluid. *Comput. Methods Appl. Mech. Engrg.* 294, 299-312
- [31]. Kandelousi, M. S. (2014). Effect of spatially variable magnetic field on ferrofluid flow and heat transfer considering constant heat flux boundary condition. *The European Phys. J. Plus*, 129- 248.
- [32]. Sheikholeslami, M., Ganji, D.D.(2015). Nanofluid flow and heat transfer between parallel plates considering Brownian motion using DTM. *Comput. Methods Appl. Mech. Eng.* 283, 651-663.
- [33]. Sheikholeslamia, M., Ganji, D. D., Javed, M. Y., Ellahi, R. (2015). Effect of thermal radiation on magnetohydrodynamics nanofluid flow and heat transfer by means of two phase model. *J. Magnetism and Magnetic Materials* 374, 36-43.
- [34]. Sheikholeslami, M., Vajravelu, K., Rashidi, M. M. (2016). Forced convection heat transfer in a semi annulus under the influence of a variable magnetic field. *Int. J. Heat and Mass Transfer* 92, 339-348
- [35]. A.C. Cogley, W.C. Vincentine, S.E. Gilles, A differential approximation for radiative transfer in a non-gray gas near equilibrium, *AIAA Journal* 6 (1968) 551-555.
- [36]. R. Grief, I. S. Habib, J. C. Lin, Laminar convection of a radiating gas in a vertical channel, *J. Fluid Mech.* 46 (1970) 513-520.
- [37]. T. Y. Na, *Computational Method in Engineering Boundary Value Problems.* Academic Press, New York, 197